

**Configurational metastable defects in irradiated epitaxially grown boron-doped  $p$ -type Si**

M. Mamor\* and M. Willander

*Physics department, Physical Electronics and Photonics, (MC2), Chalmers University of Technology and Gothenburg University, S-412 96 Gothenburg, Sweden*

F. D. Auret and W. E. Meyer

*Physics Department, University of Pretoria, Pretoria 0002, South Africa*

E. Sveinbjörnsson

*Solid State Electronics Laboratory, Department of Microelectronics ED, Chalmers University of Technology S-412 96 Gothenburg, Sweden*

(Received 25 April 2000; published 22 December 2000)

In this work, we investigate the metastability of the defect  $H\alpha 2$  introduced in epitaxially grown boron-doped  $p$ -type Si by high energy (5.4 MeV) He-ion irradiation. Deep level transient spectroscopy (DLTS) and thermally stimulated capacitance (TSCAP) measurements were used to study the electronic properties of the defect in each configuration. The analyses indicate that this metastable defect can exist in either of two configurations (A or B) and can be reversibly transformed using conventional bias-on/bias-off annealing temperature cycles. The energy barriers for transition between these two configurations (A to B and B to A) are determined as 0.79 and 0.52 eV, respectively. In addition, we have compared the electronic properties of  $H\alpha 2$  to those introduced during high-energy (12 MeV) electron irradiation and 250 keV proton irradiation. It is shown that defect  $HE2$  introduced during electron irradiation of the same epitaxially grown  $p$ -Si and a defect  $HP2$  introduced during 250 keV proton-irradiated boron doped float-zone (FZ)  $p$ -Si exhibit the same metastability as  $H\alpha 2$  and provide further evidence that  $H\alpha 2$  is hydrogen-related metastable defect.

DOI: 10.1103/PhysRevB.63.045201

PACS number(s): 71.55.-i, 61.80.Jh, 61.72.Ji, 61.72.Hh

**I. INTRODUCTION**

Most point defects in semiconductors are observed in only one configuration. However, it is possible that a defect may exist in more than one configuration, the stable configuration or a metastable configuration depending on the charge state of the defect. The alternate (metastable) configuration of a defect can be detected experimentally through its electronic properties. Under certain experimental conditions, usually bias-on/bias-off annealing cycles, the metastable defect is configurationally transformed to different energy states which can be detected by deep level transient spectroscopy (DLTS) or thermally stimulated capacitance (TSCAP) measurements. A thorough study of configurationally bistable defects in semiconductors has been reported by Levinson.<sup>1</sup>

Metastable defects are important in electronic materials because the degree to which they modify semiconductors may be reversibly altered, depending on the electric field and temperature conditions. The existence of configurationally metastable defects was first revealed by electron paramagnetic resonance (EPR) studies of the oxygen-vacancy pair in Si.<sup>2</sup> Later DLTS and TSCAP studies have also shown the presence of an unusual metastable defect in electron-irradiated  $n$ -type Si as well as in  $n$ -type GaAs and InP.<sup>3-5</sup> A defect with metastable characteristics has also been observed in boron-doped float-zone (FZ)  $p$ -Si single crystals, which is tentatively identified as the substitutional boron-vacancy complex.<sup>6,7</sup> A defect with metastable characteristics has also been detected in aluminum-doped and boron doped silicon substrates<sup>8,9</sup> following ultrafast quenching (laser irradiation). Recently, a defect with metastable characteristics has also

been detected in boron-doped, Czochralski-grown, Si that was electron irradiated at 80 K and is assumed to be the oxygen related metastable defect.<sup>10</sup> Metastable defects, however, are not limited only to the above illustrations. The DX centers in  $Al_xGa_{1-x}As$  and  $GaAs_xP_{1-x}$  (Ref. 11) also show metastable properties. It has been reported that alpha-particle irradiation also introduces a metastable defect in GaAs.<sup>12</sup> Recently, using DLTS, we observed a new metastable defect  $H\alpha 2$  introduced in boron-doped, epitaxially grown Si following room temperature alpha-particle irradiation.<sup>13</sup> This defect was found to exhibit reversible transformation between two configurations. Only in one configuration (which will be denoted as B), was the metastable defect directly observed by DLTS.

In this paper, we report the DLTS and TSCAP detection of configurationally metastable defects introduced in highly boron-doped  $p$ -Si epitaxially grown by chemical vapor deposition (CVD) following room temperature, He-ion irradiation. With new complementary investigation on this metastable defect using TSCAP, we report the observation of the metastable configuration "A." As a result, we demonstrate here evidence that the defect  $H\alpha 2$  can exist in either of two configurations designated A and B and exhibits two defect energy levels in the band gap. In order to investigate what kind of impurities might be involved in the configurationally metastable defect and the physical origin of this defect, we have compared the electronic properties of  $H\alpha 2$  to those introduced during high energy (12 MeV) electron irradiation and 250 keV proton irradiation. As a result of its electronic and metastable properties, a defect  $HE2$  introduced during electron irradiation of the same epitaxially grown  $p$ -Si and a

defect  $HP2$  introduced during 250 keV proton-irradiated boron doped float-zone (FZ)  $p$ -Si exhibit the same metastability as  $H\alpha2$ . In addition, we report on a study of the electronic properties of other defects introduced during He-ion irradiation of epitaxially grown  $p$ -Si. The He ions and electron irradiation-damage-induced defects in epitaxially grown Si are of additional interest due to the use of epitaxial materials for many devices fabrication.

In Sec. II we describe the experimental procedures involved. Section III describes the results obtained and comprises a discussion, after which some conclusions are presented in Sec. IV.

## II. EXPERIMENTAL PROCEDURES

In our research we used Schottky barrier diodes (SBD's) as the diode contact structure to the boron-doped Si. Titanium SBD's on a  $p$ -type Si layer (doped to  $6-8 \times 10^{16} \text{ cm}^{-3}$  with boron) grown epitaxially by chemical vapor deposition (CVD) on a  $p^+$  Si(001) substrate, were irradiated with high energy (5.4 MeV) He ions at a fluence of  $9.3 \times 10^{11} \text{ cm}^{-2}$ , using an Americium radio-nuclide and 12 MeV electrons at a fluence of  $1.6 \times 10^{12} \text{ cm}^{-2}$ . In addition float-zone, boron-doped samples were irradiated with 12 MeV electrons and 250 keV protons to a total dose of  $10^{13} \text{ cm}^{-2}$  and  $7 \times 10^{12} \text{ cm}^{-2}$ , respectively. DLTS, using a lock-in amplifier-based system, was used to study the defects. The bias and pulse sequence consisted of a reverse bias  $V_r$  on which pulses with amplitude  $V_p$  were superimposed. DLTS and TSCAP were also used to determine the electronic properties of the defects in each configuration, and the configurational transformation kinetics. The DLTS defect signatures (energy level in the band gap,  $E_t$ , and apparent capture cross section,  $\sigma_a$ ) were calculated from the Arrhenius plots of  $\ln(T^2/e)$  vs.  $1/T$ , where  $e$  is the emission rate at the DLTS peak temperature  $T$ . The data for the Arrhenius plots were also measured by means of an isothermal DLTS technique. Details on these experiments have been given elsewhere.<sup>13</sup>

## III. RESULTS AND DISCUSSION

In Fig. 1 we present the DLTS spectra of Si irradiated with 5.4 MeV He ions [curves (a)]. For comparison, we also include spectra recorded from identical Si samples irradiated with 12 MeV electrons at a fluence of  $1.6 \times 10^{12} \text{ cm}^{-2}$  [curves (b)]. The DLTS spectra for both samples were recorded under identical bias and pulse conditions: A filling pulse of amplitude  $V_p = 1.8 \text{ V}$  was superimposed onto a quiescent reverse bias of  $V_r = 2 \text{ V}$ . The spectra were taken after cooling the sample under zero bias (bias-off, configuration A) and after cooling with applied reverse bias (bias-on, configuration B) as shown in this figure. Curves (a) show the metastable behavior of the  $H\alpha2$  defect following He-ion irradiation. The transformation behavior of the  $H\alpha2$  level is observed after zero-bias/reverse-bias cool down cycles: cooling down the sample under zero-bias (configuration A: dotted line) causes the removal of the  $H\alpha2$  signal. Cooling down the sample under reverse-bias causes the reintroduc-

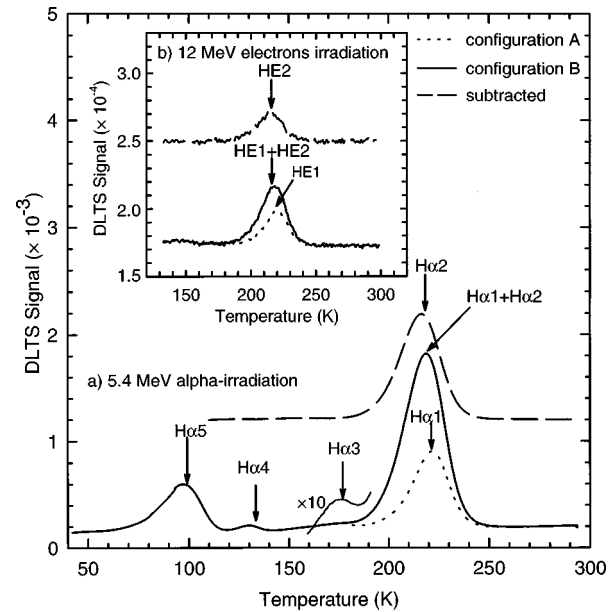


FIG. 1. DLTS spectra of  $p$ -type Si irradiated with 5.4 MeV He-ions at a fluence of  $9.3 \times 10^{11} \text{ cm}^{-2}$ , showing the result of cooling with applied zero-bias (configuration A: dotted line) and reverse-bias (configuration B: solid line). The DLTS spectrum derived from subtracting the two DLTS spectra (configuration A and B) is also shown in this curve (dashed line). The inset shows DLTS curve for 12 MeV electron irradiated  $p$ -type Si at a fluence of  $1.6 \times 10^{12} \text{ cm}^{-2}$ , showing the result of cooling with zero-bias (A) and applied reverse-bias (B).

tion of defect  $H\alpha2$  (configuration B: solid line). The DLTS peak derived from the subtraction of the two DLTS spectra for the same fluence is also shown in this curve (dashed line). The two hole traps labeled  $H\alpha1$  and  $H\alpha2$ , which are reported here, arise from two different defect levels.

The inset of Fig. 1 [curves (b)] shows DLTS spectra that characterize the two different configurations of the defect  $HE2$  following 12 MeV electron irradiation. It appears that the defects labeled  $H\alpha1$  and  $H\alpha2$  have the same signature as the defects  $HE1$  and  $HE2$ . Therefore, it is tempting to conclude that  $H\alpha1$  and  $H\alpha2$  are the same as  $HE1$  and  $HE2$ , respectively.

The temperature dependence of the hole-emission rate was studied by means of an isothermal DLTS system. The results are shown in the Arrhenius plot [Fig. 2]. In configuration A, the  $H\alpha1$  level has a hole emission activation energy of  $0.53 \pm 0.01 \text{ eV}$  and a hole capture cross section of  $(1.6 \pm 0.5) \times 10^{-13} \text{ cm}^2$ . In configuration B, peak  $H\alpha$  contains contributions of both  $H\alpha1$  and  $H\alpha2$ , and appears to have an activation energy of  $0.46 \pm 0.01 \text{ eV}$  and a capture cross section of  $(5.3 \pm 0.5) \times 10^{-15} \text{ cm}^2$ . An activation energy of  $0.43 \pm 0.01 \text{ eV}$  and a capture cross section of  $(1.4 \pm 0.5) \times 10^{-15} \text{ cm}^2$  were determined for  $H\alpha2$ . An Arrhenius plot of the thermal emission rate of the defects  $H\alpha3$  and  $H\alpha5$  is shown in the inset of Fig. 2. The DLTS signature and peak temperature of these radiation-induced defects are summarized in Table I. The signatures of  $H\alpha3$  and  $H\alpha5$  were determined under low electric-field conditions (i.e.,  $V_r = 0.3 \text{ V}$ ,  $V_p = 0.3 \text{ V}$ ). The activation energies of defects  $H\alpha3$  and  $H\alpha5$  are the same as the  $C_i-O_i$  (Ref. 14) and

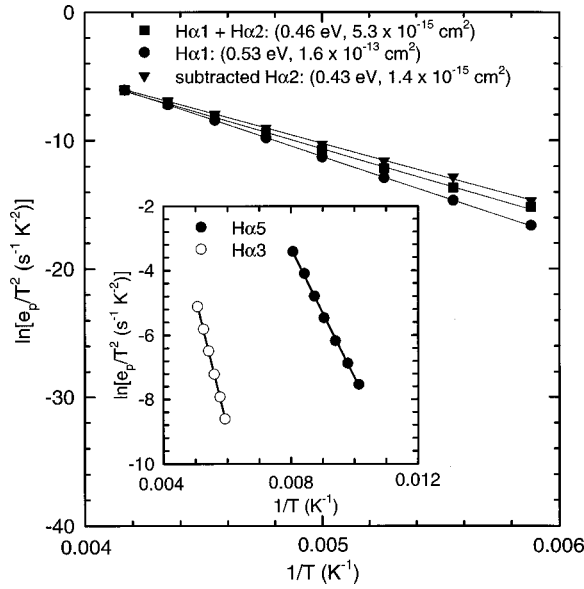


FIG. 2. Thermal emission rate data for the defect levels after cooling with bias-on (squares) and bias-off (circles). The thermal emission rate for the metastable defect is also shown (triangles). The thermal emission rates of defects  $H\alpha 3$  and  $H\alpha 5$  are shown in the inset.

divacancy<sup>15</sup> centers, respectively. A defect with a similar DLTS signature as  $H\alpha 1$  was detected;<sup>16</sup> however, the structure is as yet unresolved. The defect  $H\alpha 4$  was observed to anneal at room temperature after a few months with the appearance of a new defect  $H^*\alpha 4$  detected at  $E_v + 0.22$  eV.

Figure 3 shows DLTS scans of 250 keV proton-irradiated, FZ boron-doped,  $p$ -type Si and depicts the presence of the radiation-induced defects  $HP1$ – $HP5$ . In this study we focus on the properties of defect  $HP2$  that exhibits a metastable character. The solid line is a spectrum taken after cooling to 80 K with an applied reverse bias of 4 V applied to the sample. The temperature is then ramped up (about 5 K/min) and the spectrum is recorded. The dotted line shows a similar spectrum when the sample was cooled down to 80 K with zero bias applied to the sample. The only significant difference between the two spectra concerns the peak located at approximately 220 K, which is shifted depending on the bias during cooling. The peak has two contributions, hole emission from the state labeled B peaked at approximately 215 K (see broken line in Fig. 3) and hole emission from the state

TABLE I. Electronic properties of the prominent hole traps introduced during He-ion irradiation of epitaxially grown  $p$ -Si.

Defect label	$E_t$ (eV)	$\sigma_a$ (cm <sup>2</sup> )	Peak temperature $T_{\text{peak}}^a$ (K)
$H\alpha 1$	0.53	$1.6 \times 10^{-13}$	223
$H\alpha 2$	0.43	$1.4 \times 10^{-15}$	215
$H\alpha(H\alpha 1 + H\alpha 2)$	0.46	$5.3 \times 10^{-15}$	220
$H\alpha 3$	0.35	$2.1 \times 10^{-15}$	174
$H\alpha 5$	0.17	$1.7 \times 10^{-16}$	102

<sup>a</sup>Peak temperature at a lock-in amplifier frequency of 4.6 Hz, i.e., a decay time constant of 92.3 ms.

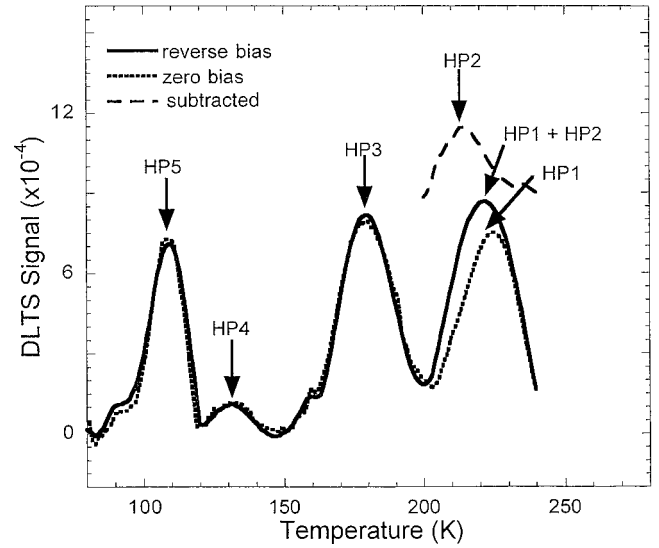


FIG. 3. DLTS spectra of a proton-irradiated, FZ,  $p$ -type silicon sample. Reverse bias=2 V, filling pulse=1.8 V and  $e_p = 10$  s<sup>-1</sup>. The broken line shows the signature of the metastable state B obtained by subtracting the dotted spectrum (zero bias during cooling) from the solid spectrum (reverse bias during cooling).

labeled A which is peaked at  $\approx 225$  K. The solid spectrum contains contributions from both states while the concentration of the B state is negligible after zero bias cooling (the dotted spectrum). The shift depends strongly upon the bias as well as the time needed to record the DLTS scan. For example if the ramp rate is reduced there is no significant difference between the two spectra and they become an intermediate between the two shown in Fig. 3. The reason for this is simply that the metastable transition takes place during the DLTS scan and a steady state between the population of the A state and the B state is reached before hole emission from the centers is recorded. The steady state ratio between the population of the states depends on the bias pulse applied during the DLTS measurement. For example, if the sample is kept at a reverse bias during the sweep and the filling pulse period is made as short as possible (10% duty cycle) the recorded spectrum is similar to the solid line in Fig. 3. If the situation is reversed and the filling pulse is on 90% of the time period, the recorded spectrum resembles the dotted line in Fig. 3. These bias-induced transformations of  $HP2$  are charge state controlled and related to a reversible disappearance and reappearance of energy levels in the band gap.

The DLTS spectra were recorded in a somewhat unusual manner to enable detection of the metastable behavior. The transition rates, at these temperatures, from the metastable state B to state A are so high that if precautions are not taken the metastability is not observed at all.

The overall results agree very well with a study of the metastable defect  $H\alpha 2$  and  $HE2$  in He-ion and electron-irradiated, epitaxially grown, boron-doped,  $p$ -type silicon, respectively. The hole emission rates of the metastable states are the same within experimental error and the bias dependence and transition rates between the metastable states are similar. Reference samples (FZ boron-doped  $p$ -type Si) from the same wafer without proton irradiation do not show any DLTS signatures of the metastable defect above the de-

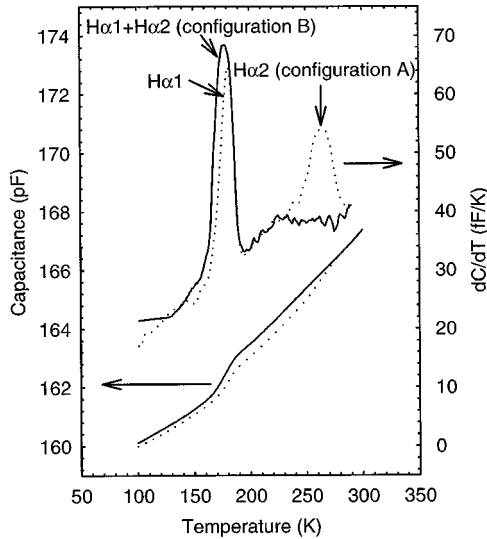


FIG. 4. TSCAP measurements of the sample shown in Fig. 1. The solid line was recorded after cooling under reverse bias while the dotted line was recorded after cooling under zero bias. In both cases the capacitance was measured at a bias of  $-1$  V and the temperature was scanned at a rate of  $3$  K  $\text{min}^{-1}$ .

tection limit which is estimated to be at a concentration of  $5 \times 10^{11} \text{ cm}^{-3}$ . The same applies to samples receiving  $12$  MeV electron irradiation using a fluence of  $10^{13} \text{ cm}^{-2}$ .

Concerning the differences in concentrations of the metastable defect after alpha irradiation as compared to electron and proton irradiation, we expect more damage with higher concentrations of point defects after high energy alpha irradiation as compared to low energy proton irradiation (only  $250$  keV) and electron irradiation. Since an alpha irradiation transfers more energy to the lattice than electron irradiation with the same kinetic energy, it is capable of forming disordered regions with a larger extent than the vacancy or interstitial defects typically observed after electron irradiation.

The remainder of this paper will concentrate on the metastability of  $H\alpha 2$  detected after He-ion irradiation. The metastability could also be observed by means of TSCAP measurements, as shown in Fig. 4. During these measurements, the sample was cooled under either zero or reverse bias in order to freeze in one of the metastable configurations of  $H\alpha 2$ . After cooling to approximately  $100$  K, a short filling pulse was applied. Here, after a reverse bias of  $-1$  V was applied, the temperature was increased at a constant rate of  $3$  K  $\text{min}^{-1}$  while the capacitance was recorded by means of an HP4192A Impedance Analyzer. Figure 4 shows the capacitance of the sample as a function of temperature, as well as its derivative  $dC/dT$ . The solid curve, which was recorded after cooling under a reverse bias of  $-1$  V, shows hole emission from both  $H\alpha 1$  and  $H\alpha 2$  (in configuration B) at about  $180$  K as a rapid increase in the capacitance of the sample and a peak in the derivative curve. The dashed curve was recorded after cooling under zero bias conditions. Here the emission at  $180$  K is due to  $H\alpha 1$  only.  $H\alpha 2$ , which has been transformed to configuration A, now emits carriers only once the temperature reaches  $265$  K, the same temperature at

which it is transformed to configuration B. This indicates that the emission of holes from  $H\alpha 2$  in configuration A is closely linked to its transformation to configuration B.

The TSCAP results indicate that the transformation from configuration A to configuration B is closely associated with the emission of a hole. However, no hole emission could be observed from configuration A by means of conventional DLTS. The possible explanation for this behavior is that if the defect transforms before hole emission takes place, the hole would be emitted immediately by configuration B, because the transformation occurs at a temperature much higher than that at which configuration B starts to emit holes. This would imply that configuration A cannot be observed by means of DLTS because it transforms to state B before emitting a hole, i.e., the ionization energy of configuration A is too high for the defect to be observed by DLTS.

The transition from one configuration to the other was investigated in more detail by studying the thermally activated transformation kinetics between configurations A and B. We used the systematic method proposed by Levinson *et al.*<sup>17,18</sup> in their study of the metastable M center in InP. In order to examine the transition  $A \rightarrow B$ , the sample was first cooled from  $300$  K to a temperature  $T$  at zero bias; then it was kept for a short time  $t$  at  $T$  under a fixed applied bias, and finally cooled rapidly to  $130$  K. The changes in the magnitude of  $H\alpha 2$  were used to determine the changing population of the defect in configuration A. In the same way, the reverse transition,  $B \rightarrow A$ , was studied using reverse-bias cooling and zero-bias annealing. Isochronal ( $5$  min) anneals were first performed to reveal the transformation temperature. The results obtained after this isochronal annealing (not shown here) revealed that both transitions  $A \rightarrow B$  and  $B \rightarrow A$  occur in only one stage, but not at the same temperature: The transformation  $A \rightarrow B$  is observed at a higher temperature ( $240$ – $265$  K) than the transformation  $B \rightarrow A$  ( $185$ – $215$  K). From our measurements, it seems that the transformation in both directions is complete. The reaction kinetics were then explored around the transformation temperatures by a series of isothermal anneals. The annealing reaction was found to be first order, as demonstrated in Fig. 5 for reaction  $A \rightarrow B$ . Here, the normalized  $H\alpha 2$  peak height is plotted as a function of anneal time and temperature. The peak height of  $H\alpha 2$  as a function of time,  $H\alpha 2(t)$ , was described by

$$H\alpha 2(t) = H\alpha 2(\infty) [1 - \exp(-R_{A \rightarrow B} t)] \quad A \rightarrow B, \quad (1)$$

$$H\alpha 2(t) = H\alpha 2(\infty) [\exp(-R_{B \rightarrow A} t)] \quad B \rightarrow A, \quad (2)$$

where  $H\alpha 2(\infty)$  correspond to a peak height with  $H\alpha 2$  completely reintroduced.

We have also measured the transformation rate from configuration A to configuration B directly with DLTS, and from B to A by varying the filling pulse width and measuring the DLTS peak height.<sup>13</sup> The kinetics for the metastable defect transitions are consistent with the following relations:

$$R_{A \rightarrow B} = 4 \times 10^{12} \exp[-(0.79 \text{ eV})/kT] \text{ s}^{-1}, \quad (3)$$

$$R_{B \rightarrow A} = 7 \times 10^9 \exp[-(0.52 \text{ eV})/kT] \text{ s}^{-1}. \quad (4)$$

Although DLTS does not provide information about the

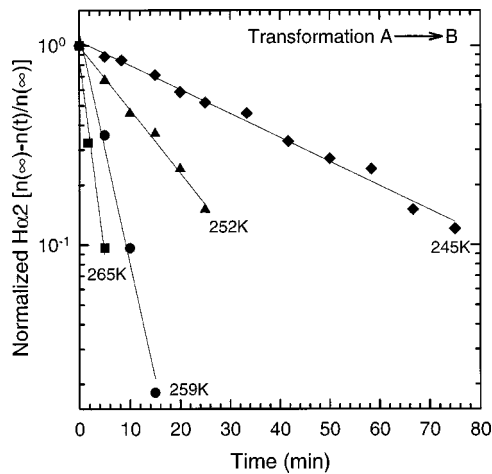


FIG. 5. Isothermal annealing kinetics for reaction A→B. For each point, the sample was cooled from 300 K to the indicated temperature with zero-bias, annealed at reverse-bias for the indicated time, and DLTS peak  $H\alpha 2$  was monitored.

physical nature of defects, we nevertheless have some indications as to what  $H\alpha 2$  may consist of. First,  $H\alpha 2$  and  $HE 2$  metastable defects have up to now been reported only in high-energy He-ion and electron-irradiated, boron-doped  $p$ -Si that was epitaxially grown by CVD and not in FZ, boron-doped,  $p$ -type Si irradiated at the same condition. Second, the same metastable defect  $HP 2$  is also observed in float-zone, boron-doped,  $p$ -Si following proton irradiation. In view of these facts we suggest that the metastable defect  $H\alpha 2$  is a hydrogen-related metastable defect due to the high concentration of hydrogen in our samples prepared by CVD and may consist of hydrogen linked to a lattice defect that was produced by the high energy bombardment.

#### IV. CONCLUSION

In summary, the results presented here demonstrate that one of the defects introduced in epitaxially grown, boron-

doped,  $p$ -type silicon by high energy He-ion and high-energy electron irradiation, exhibits charge-state controlled metastability and can be reversibly transformed using conventional bias-on/bias-off temperature cycles. This metastable defect can exist in either of two configurations (A or B). In configuration B,  $H\alpha 2$  has an activation energy  $E_t$  of  $0.43 \pm 0.01$  eV and an apparent capture cross section  $\sigma_a$  of  $(1.4 \pm 0.5) \times 10^{-15} \text{ cm}^2$ .

The physical nature of these defects can presently at best be speculated. However, in our previous study, we have observed that the defect concentration of  $H\alpha 2$  increased linearly (up to  $2 \times 10^{15} \text{ cm}^{-3}$ ) with increasing incident particle fluence, and no saturation effect has been seen for a fluence up to  $2.2 \times 10^{12} \text{ cm}^{-2}$ . The defect is either a radiation-induced complex related to impurities in the crystal of which the concentrations are higher than  $2 \times 10^{15} \text{ cm}^{-3}$ , or a lattice defect complex independent of impurities. Since the same metastable defect was produced by high-energy electron bombardment, it is likely to involve a lattice defect. The involvement of a lattice defect is also suggested by the nondetection of this metastable defect in similar materials irradiated with low-energy ions ( $< 5 \text{ keV}$ ) created by the electron beam or Ar-ion bombardment. We should also notice that these metastable defects  $H\alpha 2$  and  $HE 2$  were not observed in either He-ion or electron-irradiated, FZ boron-doped  $p$ -Si, and are present only in high-energy-particle-irradiated boron-doped,  $p$ -Si, that was epitaxially grown by CVD or in proton-irradiated, FZ boron-doped,  $p$ -Si. The overall results suggest that this defect  $H\alpha 2$  may be either an interstitial complex, or a vacancy complexed with hydrogen.

#### ACKNOWLEDGMENTS

The authors thank Dr. A. Hallen, at the Royal Institute of Technology, Stockholm, Sweden for performing proton irradiation of the samples.

\*Author to whom correspondence should be addressed. Present address: Institut für Physikalische Elektronik (IPE), Universität Stuttgart, Pfaffenwaldring 47, D-70569 Stuttgart, Germany; Electronic mail: Mohammed.Mamor@ipe.uni-stuttgart.de

<sup>1</sup>M. Levinson, J. Appl. Phys. **58**, 2628 (1985).

<sup>2</sup>G. D. Watkins, in *Lattice Defects and Radiation Effects in Semiconductors*, edited by F. A. Huntley (Institute of Physics, London, 1975), p. 1.

<sup>3</sup>O. O. Awadelkarim and B. Monemar, Phys. Rev. B **38**, 10 116 (1988).

<sup>4</sup>T. I. Kol'chenko and V. M. Lomakoi, Semiconductors **28**, 501 (1994).

<sup>5</sup>M. Stavola, M. Levinson, J. L. Benton, and L. C. Kimerling, Phys. Rev. B **30**, 832 (1984).

<sup>6</sup>C. A. Londos, Phys. Rev. B **34**, 1310 (1986).

<sup>7</sup>S. K. Bains and P. C. Banbury, J. Phys. C **18**, L109 (1985).

<sup>8</sup>A. Chantre and D. Bois, Phys. Rev. B **31**, 7979 (1985).

<sup>9</sup>A. Chantre, Phys. Rev. B **32**, 3687 (1985).

<sup>10</sup>C. A. Londos, Phys. Status Solidi A **133**, 429 (1992).

<sup>11</sup>D. V. Lang, in *Deep Centers in Semiconductors*, edited by S. T. Pantelides (Gordon and Breach, New York, 1986), Chap. 7, p. 489.

<sup>12</sup>F. D. Auret, R. M. Erasmus, S. A. Goodman, and W. E. Meyer, Phys. Rev. B **51**, 17 521 (1995).

<sup>13</sup>M. Mamor, F. D. Auret, S. A. Goodman, and W. E. Meyer, Appl. Phys. Lett. **72**, 3078 (1998).

<sup>14</sup>O. O. Awadelkarim, T. Gu, P. I. Mikulan, R. A. Ditzio, S. J. Fonash, K. A. Reinhardt, and Y. D. Chan, Appl. Phys. Lett. **62**, 958 (1993).

<sup>15</sup>B. J. Baliga and A. O. Ewaraye, J. Electrochem. Soc. **130**, 1916 (1983).

<sup>16</sup>P. K. Giri, S. Dhar, V. N. Kulkarni, and Y. N. Mohapatra, J. Appl. Phys. **81**, 260 (1997).

<sup>17</sup>J. L. Benton and M. Levinson, in *Defects in Semiconductors II*, edited by S. Mahajan and J. W. Corbett (North-Holland, New York, 1983), p. 95.

<sup>18</sup>M. Levinson, M. Stavola, J. L. Benton, and L. C. Kimerling, Phys. Rev. B **28**, 5848 (1983).